Th^{226}, Th^{228}, and Pu^{238}.[7,10] Apparently such levels are to be interpreted as octupole vibrations of a nucleus about a spheroidal shape.[7] Building on the 0^+ ground state such octupole vibrations can give rise to excited bands with $K=0^-$, 1^-, 2^-, and 3^-. From the present experiments $K=0^-$ is indicated for the 795-kev level in U^{235} as discussed in the previous section. This is in accord with the studies of neighboring nuclei which also indicate $K=0^-$ for the 1^- level.[10] Thus, the 795-kev level should probably be interpreted as the lowest member of a $K=0^-$ rotational band. Population of the higher energy states with $I=3^-$, 5^-, etc., is not expected to be appreciable in the beta decay of Pa^{234} since on the basis of log ft values the ground-state spin of Pa^{234} appears most likely to be 0.

[10] F. Stephens, Jr., F. Asaro, and I. Perlman, Phys. Rev. **100**, 1543 (1955).

ACKNOWLEDGMENTS

The author is grateful for the hospitality of the Institute for Theoretical Physics and wishes to thank Professor Neils Bohr for the excellent working conditions at the Institute. He is particularly indebted to civil igenior Sven Bjørnholm for stimulating this research and for the chemical preparation of the Th^{234} radioactivity.

PHYSICAL REVIEW VOLUME 119, NUMBER 6 SEPTEMBER 15, 1960

Elastic Scattering of Heavy Ions by Gold and Bismuth*

H. L. REYNOLDS AND E. GOLDBERG
Lawrence Radiation Laboratory, University of California, Livermore, California

AND

D. D. KERLEE
Seattle Pacific College Institute for Research, Seattle, Washington

(Received April 25, 1960)

The angular distributions of C^{12}, N^{14}, O^{16}, and Ne^{20} elastically scattered by Au^{197} and Bi^{209} have been measured at laboratory energies of approximately 10.4 Mev per nucleon. The elastically scattered ions were recorded in photographic emulsions at laboratory angles from 19° to 175°. In general, measurements were extended only to angles where the ratio of the cross section to the Coulomb cross section, σ/σ_c, was greater than 0.1. In one case the measurement was extended to a region where $\sigma/\sigma_c \leq 1.4\times10^{-4}$. The cross sections all exhibited a behavior similar to that previously reported for C^{12} on Au^{197}. An oscillation in the cross-section ratio occurring at smaller angles than the 20% to 30% rise and sudden drop was observed. Excellent agreement was obtained with the Blair "sharp-cutoff" calculations for values of $\sigma/\sigma_c > 0.2$. Nuclear interaction distances calculated by fitting the sharp-cutoff calculations are consistent with $r_0=1.46$ fermis, where $R=r_0(A_1^{\frac{1}{3}}+A_2^{\frac{1}{3}})$. No striking distinction can be made regarding the surface characteristics of the four projectiles or the two targets.

INTRODUCTION

THE study of elastic scattering of heavy ions from nuclei promises to be an important source of information concerning the size of nuclei and condition of the nuclear surface. The mean free path of nuclei heavier than α particles in nuclear matter is very small, so that the interaction is almost completely determined by the tails of the nuclear potentials and the Coulomb potential. The characteristic angular distribution obtained is best illustrated by the ratio of the measured cross section to the Coulomb cross section. It is found that at small angles this ratio is unity. As the angle increases, the ratio increases by about 20% to 30% and then falls rapidly. This same behavior was found for the elastic scattering of α particles from nuclei.[1]

A rather simple model of the interaction, the sharp-cutoff model,[2] has been applied with excellent results to the elastic scattering of nitrogen by nitrogen,[3] and carbon by gold.[4] The nitrogen-nitrogen results have been analyzed by Porter[5] using an optical model. He obtained good agreement with the experiment with a real nuclear potential of -40 Mev, an imaginary nuclear potential of -8 Mev, and a potential form factor of 6×10^{-14} cm. A good fit to the data could also be obtained by setting the real part of the nuclear phase shift equal to zero. Therefore, it is the absorption together with the Coulomb interaction which plays the major role in the elastic scattering, as would be expected because of the small mean free path in nuclear matter.

McIntyre *et al.*[6] have studied the elastic scattering

* This work was supported by the U. S. Atomic Energy Commission and by the National Science Foundation.

[1] D. D. Kerlee, J. S. Blair, and G. W. Farwell, Phys. Rev. **107**, 1343 (1957).

[2] J. S. Blair, Phys. Rev. **95**, 1218 (1954); J. S. Blair, Phys. Rev. **108**, 827 (1957).

[3] H. L. Reynolds and A. Zucker, Phys. Rev. **102**, 1378 (1956).

[4] E. Goldberg and H. L. Reynolds, Phys. Rev. **112**, 1981 (1958).

[5] C. E. Porter, Phys. Rev. **112**, 1722 (1958).

[6] J. A. McIntyre, S. O. Baker, and T. L. Watts, Phys. Rev. **116**, 1212 (1960).

TABLE I. Measured ranges and energies for the incident particles.

Reaction	Corrected range[a] (μ)	Energy at emulsion surface[b] (Mev)	Reaction energy[c] (Mev)	E/M (Hilac) (Mev)
C^{12}+Au	198.6	120.0	121.4	10.11[d]
N^{14}+Au	181.2	144.0	145.5	10.42
O^{16}+Au	159.6	162.2	164.1	10.37
Ne^{20}+Au	137.4	204.6	207.6	10.41
C^{12}+Bi	205.2	122.4	124.0	10.34
N^{14}+Bi	180.3	143.6	145.4	10.43
O^{16}+Bi	159.0	161.9	164.0	10.29
Ne^{20}+Bi	138.9	206.2	209.6	10.52

[a] These values include a 3 μ correction for rubbing of emulsions, and are based on an emulsion density of 3.815 g/cc. They are total ranges and are not corrected for grain size. The laboratory angle of scatter was approximately 20°.
[b] Values obtained using Heckman's (reference 9) range-energy data. A 0.2 μ correction was made to account for finite grain size at beginning and end of tracks.
[c] Energy at center of target before scatter.
[d] This emulsion was heavily rubbed. The value of (E/M) used in the text is 10.34 Mev/nucleon for the C^{12}+Au reaction.

of O^{16} from Au^{197}, Ni. Al^{27}, and C^{12} at a laboratory energy of 158 Mev. The results for Au and Ni are similar to the previous elastic-scattering data.[1,3,4] However, some small oscillatory structure was found before the rise in the cross section. The data for Al and C are in an angular region where $\sigma(\theta)/\sigma_c(\theta)<1$. Some diffraction structure is observed for the C^{12} data. Halbert and Zucker[7] have studied the elastic scattering of N^{14} by Be^9. Here also $\sigma(\theta)/\sigma_c(\theta)<1$. A diffraction structure is evident for these data also.

In the present paper we describe experiments concerning the elastic scattering of C^{12}, N^{14}, O^{16}, and Ne^{20} from Au^{197} and Bi^{209}. Angular distributions were measured from 19° to an angle where $\sigma(\theta)/\sigma_c(\theta)\simeq 0.1$, except for one case where $\sigma(\theta)/\sigma_c(\theta)$ was followed to 1.4×10^{-4}. The laboratory energy of the particles was approximately 10.4 Mev per nucleon. An oscillatory behavior of $\sigma(\theta)/\sigma_c(\theta)$ was observed at angles smaller than the position of the rise before the sudden drop. "Sharp-cutoff" calculations have been carried out for each of the cases, allowing a determination of the nuclear interaction radius for all of the nuclei involved. The sharp-cutoff calculations are in excellent agreement with the data.

EXPERIMENTAL PROCEDURE

The experimental arrangement has been described in a previous paper.[4] A collimated beam of particles struck a thin unsupported target of gold (0.75 mg/cm²) or bismuth (0.9 mg/cm²). The scattered particles passed on to nuclear emulsions, while the main beam proceeded into a collector cup. Integrated charges of approximately 4×10^{-6} coulombs were collected for each exposure. The beam from the Hilac was deflected either 15° or 30° by a bending magnet before reaching the target. The targets were placed approximately 3 meters from the magnet and were at an angle of 60° with respect to the beam axis. There were no absorbing foils between the Hilac and the target. The magnet used for background suppression, as described in the previous paper,[4] was not used, although lead absorbers were placed about the chamber for reducing x-ray background. Some surface blackening of the emulsions occurred and was removed by gently rubbing the surfaces.[8] This rubbing removes about one micron of the emulsion depth, as will be discussed later. *K-O* emulsions, 200 μ thick, were used for all exposures. The emulsion density after 45 minutes in vacuum was 3.94 g/cc.

The number of tracks per unit area was determined with a standard Leitz binocular microscope and an eyepiece reticle. The scattering angle and geometric correction factors were found from measurements of the geometry of the scattering chamber, and are presented in the previous paper.[4] The emulsion holders, target, and collimator were all mounted permanently on a single plate so that changes in geometry could not occur during the experiment.

The beam was collimated by two slits $\frac{1}{32}$ in.$\times\frac{1}{2}$ in., placed $7\frac{1}{2}$ in. apart. In the case of N^{14} and Ne^{20} on Bi^{209},

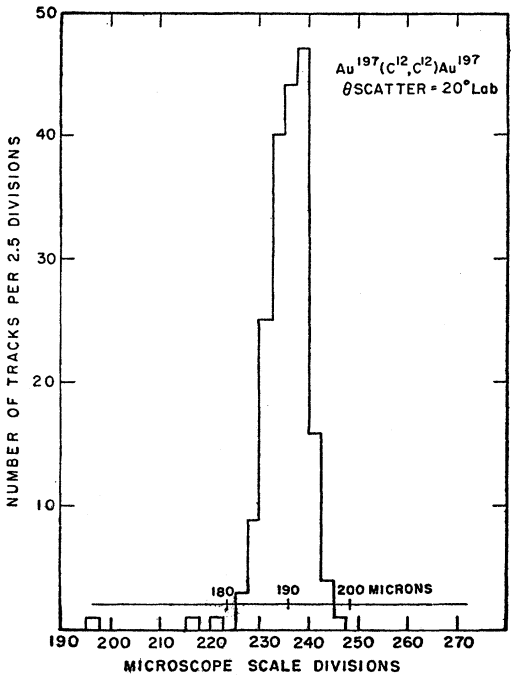

FIG. 1. A typical range spectrum in emulsion for carbon ions elastically scattered from gold at a scattering angle of 20° in the laboratory. Emulsion density is 3.94 g/cc. The micron scale has been corrected for track dip angle in the emulsion.

[7] M. L. Halbert and A. Zucker, Phys. Rev. **115**, 1635 (1960).

[8] Since the exposures were made, we have determined, with the cooperation of J. T. Gilmore, that the blackening of the emulsion surface is almost entirely due to δ rays (recoil electrons) created by the beam passing through the target. This source of background has been eliminated in subsequent exposures by straddling the target with a permanent magnet having a field strength of about 1 kilogauss. This gives a radius of curvature of $\frac{1}{2}$ cm to 22-kev electrons, the maximum expected energy, and a radius of 10 meters to the heavy ions, causing an angular deflection of approximately 0.1 degree for the heavy ions. The electrons cannot cross the field to the plates. Plates exposed using this magnet have little surface blackening.

the slits were $\frac{1}{4}$ in. in height. These slits are one-half as wide as those used in the previous experiment. Errors in the scattering angle, θ_{sc}, arise from several sources and depend upon the value of θ_{sc}. In the present chamber, the cumulative effect of the errors is near maximum at a θ_{sc} of approximately 35°. The discussion below pertains to a range of scattering angles of 30°–40°.

The uncertainty of the scattering angle is important due to its relation to the cutoff (l') value in the sharp-cutoff calculation which leads to the interaction distance, R. However, effects that simply cause a spread in scattering angle, such as multiple scattering in the target and finite target width, influence the angular resolution but not the uncertainty in the l' determination.

The finite width and height of the collimator account for an angular spread of ±0.6° (i.e., full width at half maximum of 1.2°). The area of the target that is illuminated is expected to be greater than the collimator area because of the allowable divergence of the beam that falls on the collimators. The above value also includes the direct effect on scattering angle of the beam divergence. In addition, the collimator height contributes to an error in the average scattering angle.[4] For the $\frac{1}{2}$-in. high collimators, the true scattering angle is 0.35° greater than the nominal scattering angle, whereas the shift is only 0.1° for the $\frac{1}{4}$-in. high collimators. Multiple scattering in the target contributes ±0.4°. The finite length of the swath scanned on the emulsion was limited to less than 6 mm and so contributed insignificantly to the angular spread.[4]

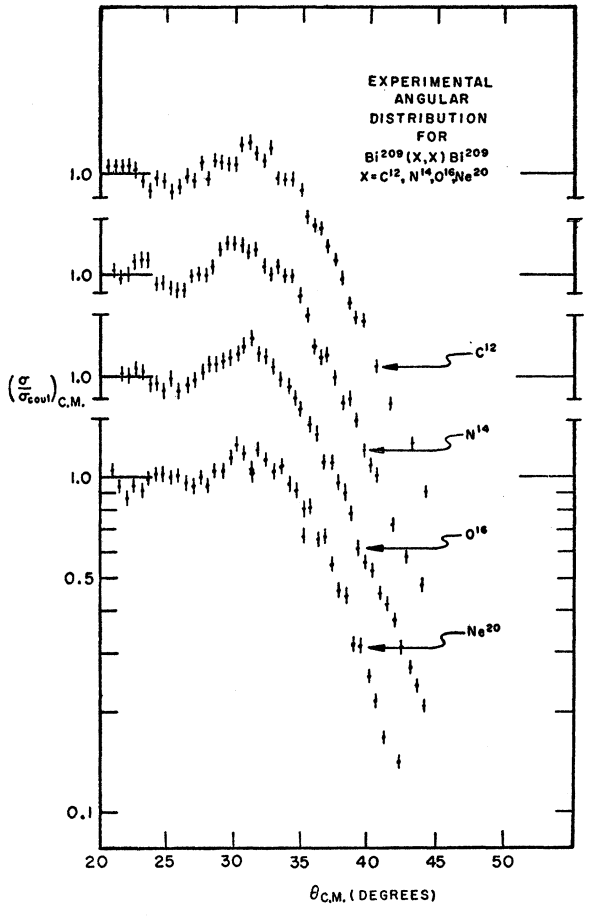

FIG. 2. Ratio of the differential cross section for elastic scattering to the Coulomb cross section versus the center-of-mass scattering angle for C^{12}, N^{14}, O^{16}, and Ne^{20} scattered by Bi^{209}. The energy of the incident ions is given in Table I. The curves have been normalized to unity at small angles.

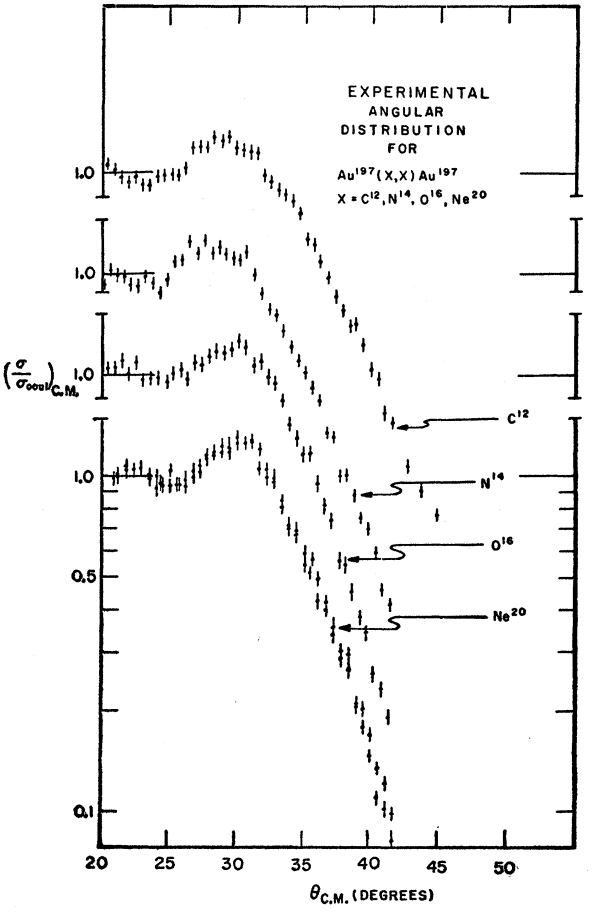

FIG. 3. Ratio of the differential cross section for elastic scattering to the Coulomb cross section versus the center-of-mass scattering angle for C^{12}, N^{14}, O^{16}, and Ne^{20} scattered by Au^{197}. The energy of the incident ions is given in Table I. The curves have been normalized to unity at small angles.

The spread in beam energy is also reflected as a loss in angular resolution. This effect was evaluated previously[4] by means of the sharp-cutoff calculation. A spread in energy of 1.7 Mev leads to a spread in angular resolution of 0.7° for 120-Mev C^{12} ions on Au^{197}. For 200-Mev Ne^{20} ions on Au^{197}, a 2.8-Mev spread leads to the same angular resolution. The energy spread which is determined below leads to ±0.5° for all reactions.

These factors yield a resultant spread in scattering angle of ±0.9° (i.e., 1.8° full width at half maximum). As a consequence, fine structure in the angular distri-

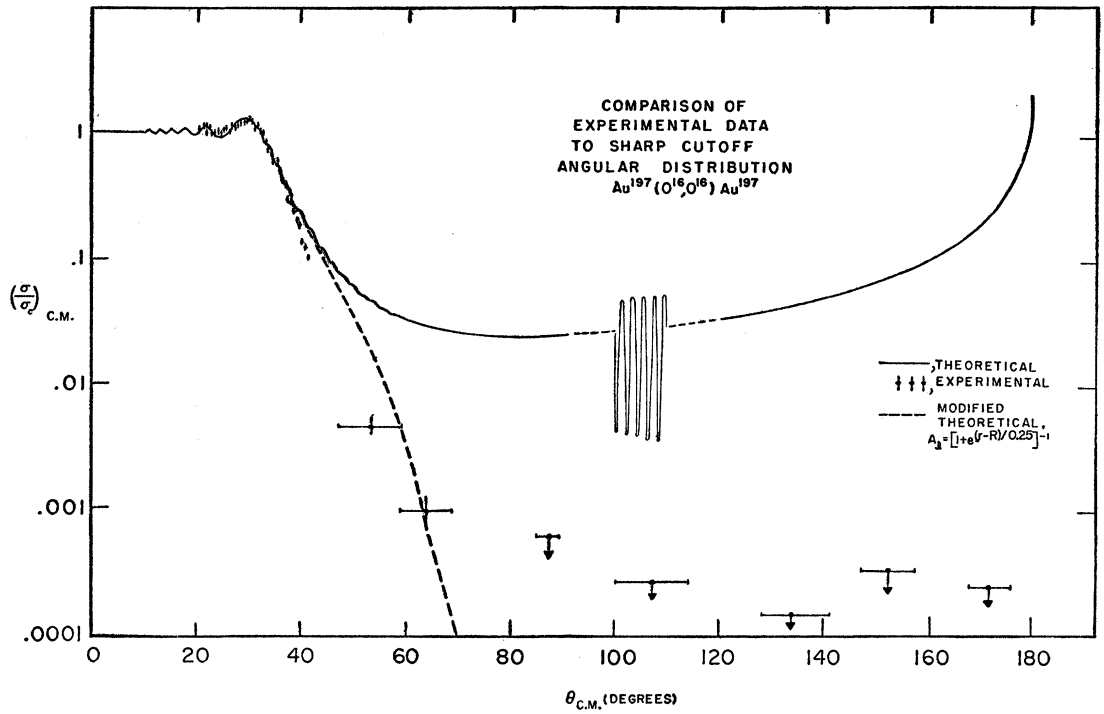

FIG. 4. Ratio of the differential cross section for elastic scattering to the Coulomb cross section versus the center-of-mass scattering angle, for O^{16} scattered by Au^{197}. The laboratory energy before scatter was 164 Mev. The solid curve was calculated by the sharp-cutoff method with $l'=89$. The fine structure for the calculation is reproduced only between 100° and 110°. The dashed curve is the result of a modified sharp-cutoff. Experimental points beyond 80° are upper limits only.

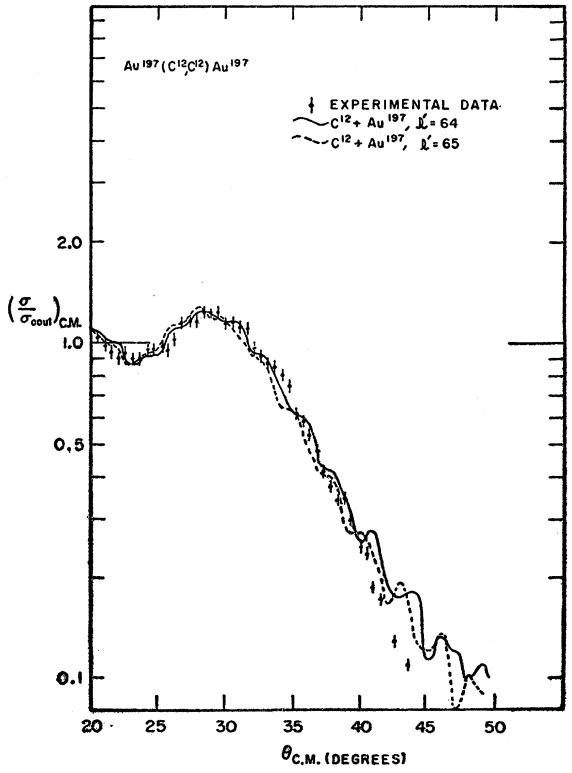

FIG. 5. Ratio of the differential cross section for elastic scattering to the Coulomb cross section versus the center-of-mass scattering angle, for C^{12} scattered by Au^{197}. Sharp-cutoff calculations are shown for cutoff l' values of 64 and 65.

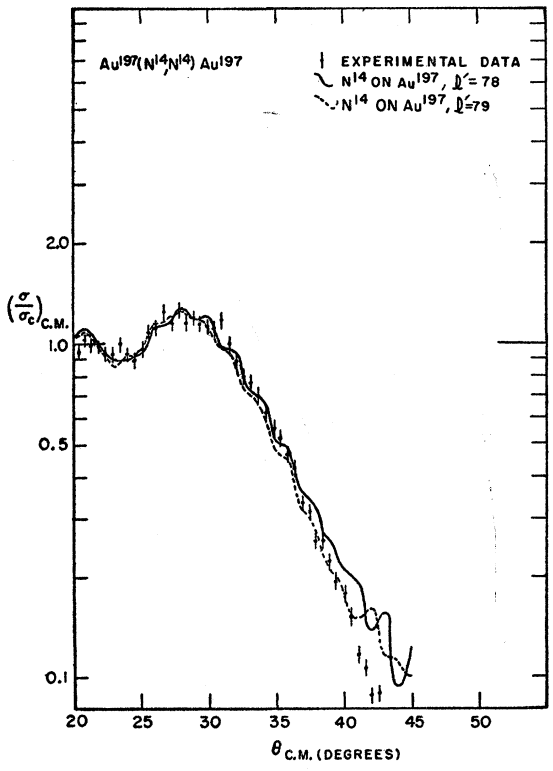

FIG. 6. Ratio of the differential cross section for elastic scattering to the Coulomb cross section versus the center-of-mass scattering angle, for N^{14} scattered by Au^{197}. Sharp-cutoff calculations are shown for cutoff l' values of 78 and 79.

bution with a width of a few degrees or less is expected to be strongly distorted.

The positions of emulsions, target, and collimators were measured with respect to scribed lines on the chamber base. The error in angle due to these measurements was $\pm 0.7°$. This latter uncertainty enters into the determination of the uncertainty in the cutoff l'. Also, the finite collimator height requires a correction to the scattering angle, which implies a correction to l'.

The energy of the heavy ions was determined by measuring range spectra at a few angles for each exposure. Three microns were added to each of the ranges to correct for rubbing of emulsions. The correction is discussed below. The range-energy curves of Heckman *et al.*,[9] were used to determine the ion energies. The ranges and laboratory energies for scattering from the bismuth and gold targets are given in Table I.

Recent exposures to fission fragments from the $N^{14}+Bi^{209}$ and $Ne^{20}+Bi^{209}$ reactions allowed a comparison of fragment ranges between plates that were shielded from δ rays by the magnetic suppressor[8] and plates that were not. The latter included those that furnished data for the present work. This comparison showed that approximately three microns of track length of these tracks that entered the emulsions at a laboratory angle of 20° were removed by rubbing. Observation of the fission-fragment range, rather than that of heavy ions, proved to be more convenient as well as more reliable. for estimation of the range loss due to rubbing.

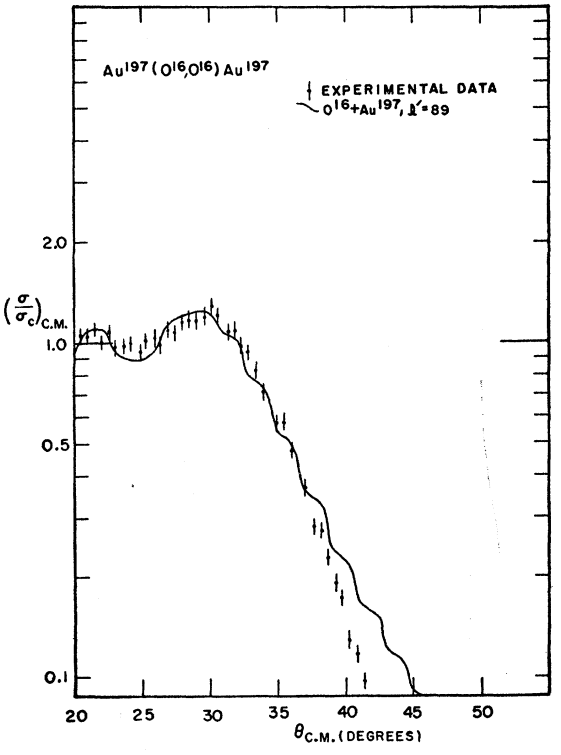

FIG. 7. Ratio of the differential cross section for elastic scattering to the Coulomb cross section versus the center-of-mass scattering angle, for O^{16} scattered by Au^{197}. A sharp-cutoff calculation for a cutoff l' value of 89 is shown.

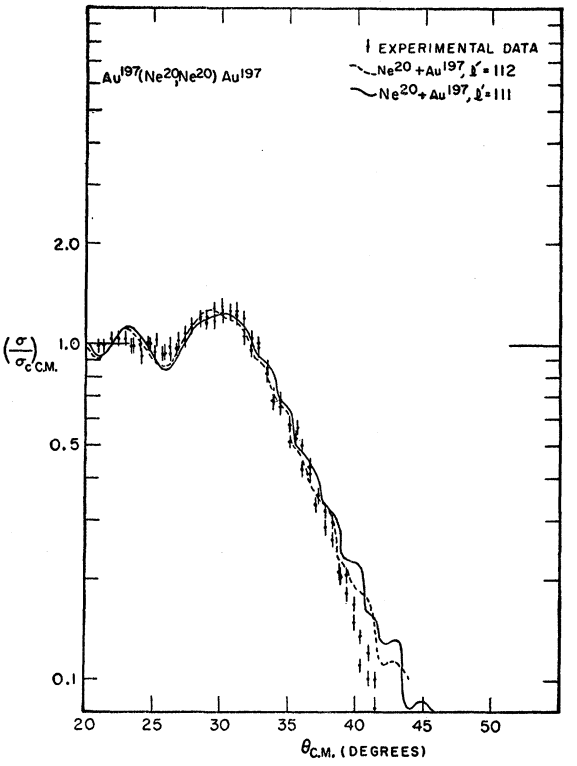

FIG. 8. Ratio of the differential cross section for elastic scattering to the Coulomb cross section versus the center-of-mass scattering angle, for Ne^{20} scattered by Au^{197}. Sharp-cutoff calculations are shown for cutoff l' values of 111 and 112.

A typical range spectrum is shown in Fig. 1 for C^{12} on Au^{197} at a laboratory scattering angle of 20°. The straggling observed in Fig. 1 gives a standard deviation of 1.6%, part of which arises from range straggling. The range straggling is approximately 1.0%,[9] leaving 1.3% in range which is due to the energy spread of the analyzed Hilac beam and energy loss in the target. From range-energy curves,, one finds that this range spread is equivalent to a 0.8% spread in energy. The target does not contribute perceptibly to the spread because the total energy loss in the target is practically independent of the depth at which scattering occurred. Therefore, the energy spread of the beam entering the chamber has a standard deviation of 0.8%.

For the $C^{12}+Au^{197}$ reaction the target was 0.6 Mev thick, which gives a spread in interaction energy of $\simeq\pm 0.3$ Mev, or $\pm 0.25\%$. For the $Ne^{20}+Au^{197}$ reaction, the target thickness was 1.7 Mev, which implies a spread of $\pm 0.4\%$. It is clear, therefore, that the spread in interaction energy is determined almost completely by the spread in beam energy. The resultant standard deviation for the C^{12} energy is 1.0 Mev, and that of the Ne^{20} beam is 1.6 Mev. Therefore the standard deviation

[9] H. H. Heckman, B. L. Perkins, W. G. Simon, F. M. Smith, and W. H. Barkas, Phys. Rev. **117**, 544 (1960).

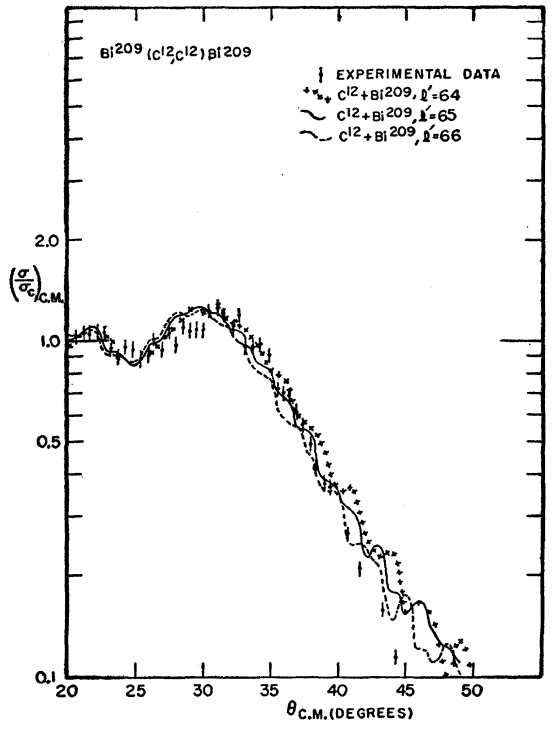

FIG. 9. Ratio of the differential cross section for elastic scattering to the Coulomb cross section versus the center-of-mass scattering angle, for C^{12} scattered by Bi^{209}. Sharp-cutoff calculations are shown for cutoff l' values of 64, 65, and 66.

of the effective angular spread due to the energy spread is 0.4° for both reactions.

Absolute cross sections were not measured. However, at small angles the scattering cross section is due to Coulomb scattering. Thus the angular distribution can be normalized to the Coulomb cross section at small angles.

RESULTS

The results of the experiment are given in Figs. 2 and 3. Laboratory energies of the respective projectiles before scatter at the center of the Au and Bi targets are listed in Table I. The ratio of the differential cross section in the center-of-mass system to the Coulomb cross section in the center-of-mass system is plotted versus the scattering angle in the center-of-mass system. For purposes of normalization, it has been assumed that the ratio approaches unity as the angle of scatter decreases. Each point represents 300 tracks, with a resulting standard deviation of approximately 6%.

Broadening of the experimental-range spectrum in the region $\sigma/\sigma_c \cong 0.1$ due to nonelastic events was corrected for by using a spectral shape determined at smaller angles and rejecting tracks outside of the proper spectrum.

One angular distribution, Au^{197} (O^{16}, O^{16}) Au^{197}, was extended to large angles (Fig. 4). Tracks comprising the data at 53° and 64° were individually analyzed for range and density to eliminate obvious inelastic events and products of fragmentation. The ratio σ/σ_c at 64° is shown to be at most 9.5×10^{-4}, or $\sigma(64°) \leq 2.6\times10^{-28}$ cm². At 87°, 106°, and 134° tracks were seen of the correct range, but with a reduction of density of approximately 30%: no tracks were seen with the required range and density. Hence upper limits to the elastic scattering are indicated at these points. At 152° and 171° within a comparable solid angle no tracks of the proper range were seen. The acceptance angle for these points was deliberately broadened, as indicated in Fig. 4, in order to obtain improved sensitivity. At 171°, $\sigma(171°) < 4\times10^{-30}$ cm².

DISCUSSION

Sharp-cutoff calculations have been made for each of the experimental curves. The method has been described in a previous paper.[4] It is assumed that if the potential barrier of the lth wave allows the particles to overlap, the outgoing lth wave is destroyed. The largest l value to be destroyed is termed the "cutoff l'." The experimental data are presented in Figs. 5 through 12, together with sharp-cutoff calculations for appropriate l' values. Excellent agreement with experiment is obtained with the calculations for values of $\sigma/\sigma_c > 0.2$. The heavy-ion scattering exhibits a much stronger absorp-

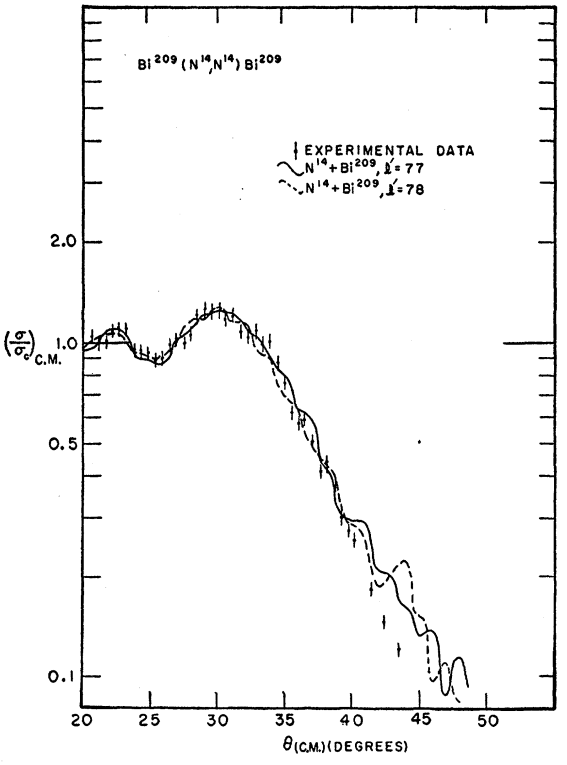

FIG. 10. Ratio of the differential cross section for elastic scattering to the Coulomb cross section versus the center-of-mass scattering angle, for N^{14} scattered by Bi^{209}. Sharp-cutoff calculations are shown for cutoff l' values of 77 and 78.

tion than similar alpha-particle scattering.[1] Consequently, in the heavy-ion experiments, the oscillations preliminary to the major rise, predicted by the sharp-cutoff model, may be seen with some detail. These oscillations were not seen in our earlier work.[4]

The experimental cross-section ratio decreases more rapidly with increasing angle for values of $\sigma/\sigma_c<0.2$ than the sharp-cutoff model predicts. In Fig. 4, the sharp-cutoff calculation is shown from 20° to 180°. The solid curve is calculated for $l'=89$. Between 100° and 110°, points were computed every $\frac{1}{4}$° to show the rapid oscillations which appear. Because of the poor resolution of the experimental points beyond 42°, these oscillations would not be observed if they did exist. The data show no evidence for a rise in the cross-section ratio at backward angles of scatter. Recently, McIntyre *et al.*[10] have shown, contrary to previous results,[11] that modified sharp-cutoff calculations can reproduce the sharply falling cross-section ratio for values of $\sigma/\sigma_c<0.2$. The modified sharp cutoff also eliminates the rapid oscillations at larger angles. Confirmation is seen in Fig. 4 as the modified theoretical curve. The calculation was performed by modifying the amplitudes of fifteen

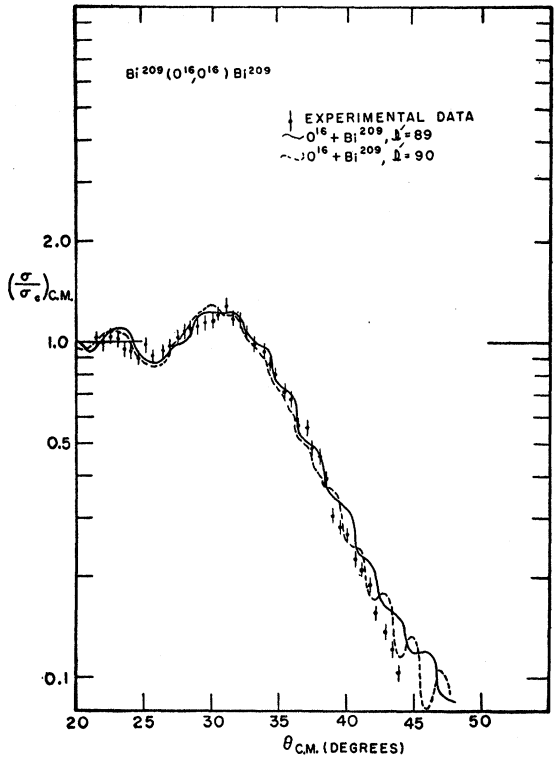

FIG. 11. Ratio of the differential cross section for elastic scattering to the Coulomb cross section versus the center-of-mass scattering angle, for O^{16} scattered by Bi^{209}. Sharp-cutoff calculations are shown for cutoff l' values of 89 and 90.

[10] J. A. McIntyre, K. H. Wang, and L. C. Becker, Phys. Rev. **117**, 1337 (1960).

[11] N. S. Wall, J. R. Rees, and K. W. Ford, Phys. Rev. **97**, 726 (1955); R. E. Ellis and L. Shecter, Phys. Rev. **101**, 636 (1956).

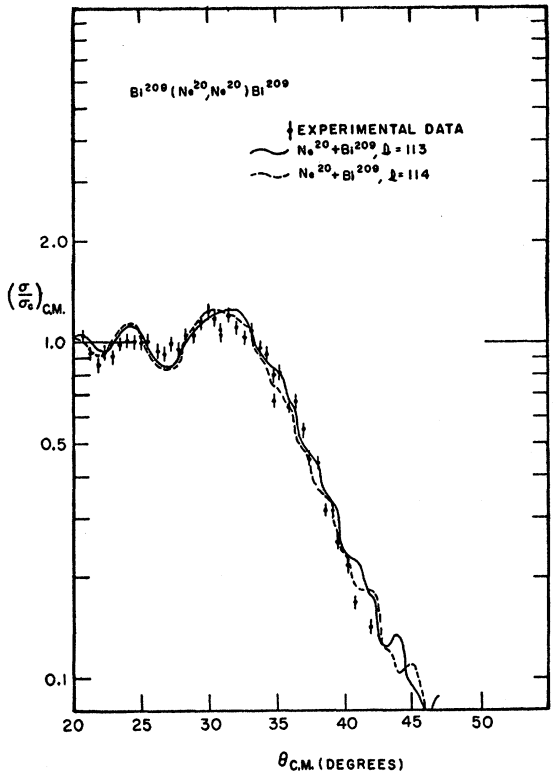

FIG. 12. Ratio of the differential cross section for elastic scattering to the Coulomb cross section versus the center-of-mass scattering angle, for Ne^{20} scattered by Bi^{209}. Sharp-cutoff calculations are shown for cutoff l' values of 113 and 114.

partial waves, as represented in the Blair expression[4] in the following way:

$$A_l=\{1+\exp[(l-l')/2.73]\}^{-1}.$$

This is equivalent to the form:

$$A_r=\{1+\exp[(r-R)/0.25]\}^{-1}.$$

The sharp-cutoff calculations were fitted to the data in the region $0.4\leq\sigma/\sigma_c\leq1.0$. As explained in an earlier paper,[4] it is expected that in this region the calculation

TABLE II. Cutoff l' values and nuclear interaction distances inferred from the sharp-cutoff model.

Reaction	Cutoff l'[a]	Interaction distance, R (fermis)[b]	r_0 (fermis)
$C^{12}+Au^{197}$	64.0±1.5	11.7±0.2	1.45±0.03
$N^{14}+Au^{197}$	78.0±1.7	12.1±0.2	1.47±0.03
$O^{16}+Au^{197}$	88.0±2.1	12.25±0.2	1.47±0.03
$Ne^{20}+Au^{197}$	112.0±2.8	12.5±0.2	1.47±0.03
$C^{12}+Bi^{209}$	64.5±1.5	12.0±0.2	1.45±0.03
$N^{14}+Bi^{209}$	77.0±1.7	12.1±0.2	1.45±0.03
$O^{16}+Bi^{209}$	89.5±2.1	12.6±0.2	1.49±0.03
$Ne^{20}+Bi^{209}$	113.0±2.8	12.7±0.2	1.45±0.03

[a] The error is the probable error. In addition to the uncertainty in fit to theory, the uncertainty in θ_{sc} due to chamber geometry is included.
[b] The error is the probable error.

TABLE III. Values of constants in error determination for interaction distance.

Projectile	a (fermis/Mev)	b (fermis)
C^{12}	−0.100	+0.130
N^{14}	−0.093	+0.108
O^{16}	−0.084	+0.092
Ne^{20}	−0.059	+0.073

should best reproduce the data. After finding the best-fit l' values, nuclear interaction distances, R, were obtained from the equation

$$E_{\text{c.m.}}=\frac{Z_1Z_2e^2}{R}+\frac{\hbar^2l'(l'+1)}{2\mu R^2},$$

where μ is the reduced mass. The results are shown in Table II. The value of $E_{c.m.}$ in the above equation was the nonrelativistic energy corresponding to the measured (slightly relativistic) energy ($E_{c.m.R}$), where $E_{c.m.}=0.984\,E_{c.m.R}$. Also, the reduced mass was determined from the rest mass of the particles. This action was taken because the sharp-cutoff model is nonrelativistic, and proper comparison of the data to calculated angular distributions necessitates the use of a common frame of reference. Since $\beta=0.148$, the correction to the interaction distance for relativistic effects is expected to be less than a few percent. Values of r_0 were obtained from the relation $R=r_0(A_1^{\frac{1}{3}}+A_2^{\frac{1}{3}})$.

The error in the radius was determined by the relation

$$|dR|^2=|adE_{c.m.}|^2+|bdl'|^2.$$

The constants a and b are shown in Table III. The magnitude of dl' is determined from the uncertainty in scattering angle, as well as the uncertainty in l', from fitting the curves to the data. The term involving dE includes a small contribution due to the fact that a wrong energy choice for the sharp-cutoff fitting will give an error in l'. Otherwise, the constants a and b were determined from the above relation between E, R, and l'. The value of r_0 is consistent with 1.46 for all of the reactions. The interaction distance for C^{12} on Au was determined previously[4] at approximately 118 Mev to be 11.8±0.3 fermis, which is in good agreement with the present experiment.

The presence of the major rises equal to or nearly equal to those predicted by the sharp-cutoff model indicates that no striking distinction can be made regarding the surface characteristics of the four projectiles or two targets in this experiment. There is a need for further study of elements where greater differences might be expected.

ACKNOWLEDGMENTS

We wish to thank the operating crew of the Hilac for their cooperation during the exposures. We are indebted to Mr. George Leipelt for processing the emulsions, and to our scanners, Mrs. Doris Irwin, Charles Chiu, James Crichton, David Corey, and Paul Hsu. The targets were prepared by Dan O'Connell. We are indebted to Dr. T. C. Merkle for his support and encouragement, and to Dr. J. S. Blair for interesting discussions of the experiment.